Real-time spectroscopy of novel solid-state random lasers

Sara García-Revilla[a], Joaquín Fernández*[a,b], Rolindes Balda[a,b], Marcos Zayat[c], David Levy[c]
[a]Dept. Física Aplicada I, Escuela Técnica Superior de Ingeniería, Alda. Urquijo s/n 48013 Bilbao, Spain
[b]Unidad Física de Materiales CSIC-UPV/EHU and Donostia International Physics Center, Apartado 1072, 20080 San Sebastián, Spain
[c]Instituto de Ciencia de Materiales de Madrid-ICMM, CSIC Cantoblanco, 28049 Madrid, Spain

ABSTRACT

Herein we report efficient random lasing in two powder samples containing rhodamine 6G (Rh6G) doped SiO_2 nanoparticles which are either directly dispersed within pure silica particles or embedded in a silica gel matrix which is subsequently ground. Basic properties of random lasing such as emission kinetics, emission spectrum, and stimulated emission threshold are investigated in both novel solid-state materials by real-time spectroscopy. The laser-like emission dynamics of the ground powder obtained out of a bulk silica gel containing 2% Rh6G-SiO_2 nanoparticles was accurately described by a light diffusive propagation model. The device behavior is close to a conventional ultrafast Q-switched laser, which is a very interesting feature aimed to further applications.

Keywords: Laser materials, time-resolved spectroscopy, random lasing, ultrafast lasers

1. INTRODUCTION

Since 1967 when Letokhov theoretically predicted lasing in random media [1], investigations concerning light amplification in locally inhomogeneous dielectric materials have resulted in the development of a new fascinating research field which gathers fundamental aspects of both classical and quantum optics together. It is only recently that researchers have started to fully understand the physical mechanisms behind general signatures of random lasing such as an overall spectral narrowing (with the eventual presence of narrow spikes in the emission spectrum), a threshold behavior, and an output pulse shortening. An overview of latest results and theories describing random lasers has been recently reported [2]. Note that the specific feedback mechanism and behavior of each of these amplifying disordered systems depend on its nature and morphology [3-5]. The wide variety of random lasers materials studied so far explains the lack of a unique theoretical treatment for all of them [6-9]. In particular, experimental observation of random lasing has been reported in material systems ranging from rare-earth powder, liquid dyes, polymer films, semiconductor nanoparticles, liquid crystals, human tissues, etc (see Refs. [2-4] and references therein). Nevertheless, much care is needed when comparing results from different random laser experiments because they can be influenced by experimental conditions such as the boundaries imposed by the sample holder, the way in which the sample is excited or light emission collected [10,11].

In this paper, we present a detailed real-time spectroscopic study in two novel solid-state materials containing SiO_2 nanoparticles embedding Rh6G. The interest of this study is two fold. On the one hand, few examples of random laser experiments have been reported in the literature where measurements were carried out in the spectral and time domain [12-18]. On the other hand, only a few random lasers have been conducted by embedding a dye in a solid host [17,19-22]. In fact, within the class of dye random lasers, laser-like action has been mainly demonstrated in a solution with external scatterers. In a very recent paper, we presented experimental results of random lasing in a ground powder made of a silica gel containing Rh6G doped nanoparticles [23]. Here, we compare the random laser behavior of this novel organic-inorganic hybrid material with a powder sample containing the same fluorescent nanoparticles directly dispersed within undoped SiO_2 nanoparticles by using ultrafast time-resolved spectroscopy. Note that both solid-state systems have a quenched disorder contrarily to classical liquid dye random lasers. Moreover, we have shown that a light diffusive propagation model can accurately describe the laser emission dynamics found in this kind of disordered active systems. The temporal analysis of the light emitted above threshold clearly suggests a behavior which is similar to a laser device working in a Q-switch-like regime.

Optical Components and Materials VI, edited by Shibin Jiang, Michel J. F. Digonnet, John W. Glesener, J. Christopher Dries, Proc. of SPIE Vol. 7212, 72120K

2. EXPERIMENTAL

2.1 Synthesis and characterization of the laser samples

Two powder laser samples (A and B) based on rhodamine 6G doped silica nanoparticles (~ 10 nm) were prepared via the sol-gel method in a two-step procedure. In a first stage, the Rh6G doped SiO_2 nanoparticles are synthesized. These fluorescent nanoparticles are then either dispersed within pure silica nanoparticles (sample A) or embedded in a silica matrix to obtain a doped silica gel which is subsequently ground (sample B). A detailed description of the synthesis procedure is given below.

The fluorescent nanoparticles were prepared by dissolving rhodamine 6G in ethanol ($6.6x10^{-3}$M) and the subsequent addition of tetraethoxysilane (TEOS) to obtain a Rh6G/TEOS ratio of 0.022. The solution was stirred prior to the addition of 1M ammonia solution (ammonia/Si = 0.174). The resulting mixture was vigorously stirred for one hour, and then 10 mL of 0.269M TEOS in ethanol solution were added to 17 mL of the previously prepared solution, followed by the addition of 3.8 mL of 0.206M ammonia solution. The solution was allowed to hydrolyze under vigorous stirring and then stabilized for the precipitation of the Rh6G doped SiO_2 nanoparticles. After separation from the supernatant liquid and drying, the dye-doped particles were ready for the next step of the procedure.

The R6G doped silica nanoparticles were mixed with undoped SiO_2 from Cab-o-sil to obtain a 2% in weight of R6G-doped particles dispersed in silica nanoparticles. After the addition of a minor amount of ethanol, the mixture was placed in an ultrasonic bath to allow the de-aggregation of the particles, and obtain a homogenous mixture. The sample was then allowed to dry and the resulting powder was ground again in a mortar before performing the measurements.

For the preparation of the doped silica gel, sample B, 2 wt% of the previously prepared Rh6G-SiO_2 nanoparticles were dispersed in ormosil sols to form the fluorescent particles doped hybrid gel, which was finally dried at 50 ºC for two weeks. In order to obtain ground powder out of the silica gel containing 2% Rh6G-SiO_2 nanoparticles, a mixer mill (Retsch MM200) was employed during 4 min. The polydispersity of the measured powder was evaluated from SEM (scanning electron microscope) photographs (see Fig. 1(a)). The particle size was estimated from the average between the major and minor axis lengths of the grains. Fig. 1(b) shows the corresponding particle size histogram. By fitting the histogram to a log-normal function an average powder size of 3 ± 1.2 μm was obtained.

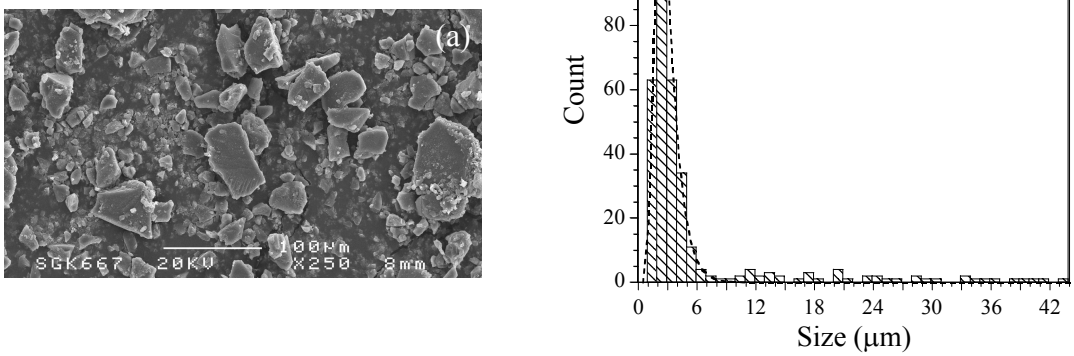

Fig. 1. (a) Scanning electron microscope photograph of the ground powder of a bulk silica gel containing 2% Rh6G-SiO_2 nanoparticles. (b) Particle size histogram of the grains. The dashed line corresponds to the log-normal fit from which an average particle size of 3 ± 1.2 μm is calculated.

Both powder laser samples were compacted in a quartz cell for handling ease and optical characterization. The volume filling factor of the powder materials was calculated by measuring sample volume and weight.

Thickness dependence of diffuse transmittance was evaluated in the ground powder of the silica gel containing 2% Rh6G-SiO_2 nanoparticles in order to experimentally determine the corresponding transport mean free path (l_t) [24,25]. The absolute diffuse transmittance spectra of the ground powder with less than 500 μm sample thickness were measured in a Cary 5 spectrometer with an integrated sphere assembly. The transmission measurements of those samples with a

larger thickness (up to 2.5 mm) were acquired by using a narrow-angle arrangement. In this case, a diode laser at 656 nm was used as the excitation source and the transmitted light was detected by means of a photomultiplier connected to a lock-in amplifier. The estimated value of l_t was 9.5 ± 0.5 μm for a wavelength of 656 nm.

2.2 Experimental techniques

The spectral and temporal measurements were performed at room temperature in a backscattering arrangement by using the frequency doubled output (532 nm) of a 10 Hz, Q-switched Nd: YAG laser as the excitation source (see Fig. 2). The pump pulse duration was 40 ps. The laser excitation energy was attenuated with a pair of polarizers and measured with an energy meter. The laser beam was impinged on the sample at normal incidence with a spot size of 2 mm after reflection from a dicroic mirror. Ground powder was compacted in a 6 mm high cylindrical cuvette with no front cell window. This sample holder has a diameter size larger than the incident laser spot (6 mm and 2 mm, respectively). The emission from the free sample surface was collected along the backward direction of the incident pump beam with an optical fiber by use of two lenses. This geometry, also used to perform temporal measurements, is particularly useful to reduce reflection effects of the pump and emitted radiation in the cuvette walls. A long-pass filter was used to remove light at the pump frequency.

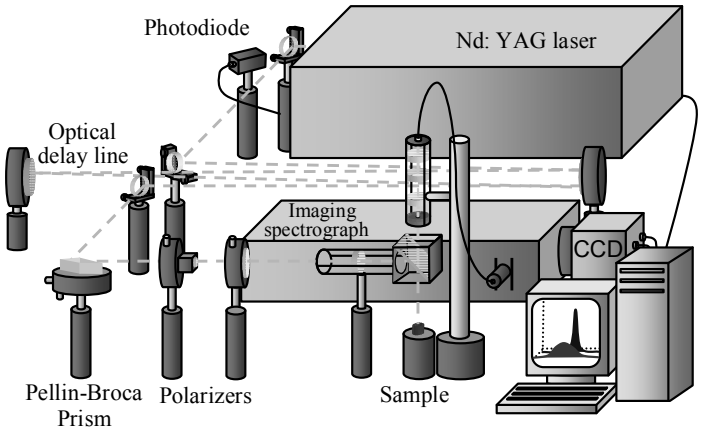

Fig. 2. Experimental set-up for time-resolved spectroscopy measurements.

In the spectral measurements, the emitted light was dispersed by a 0.5 m imaging spectrograph and recorded by a gated intensified CCD camera. This camera allows time-resolved detection of luminescence with exposure times down to 200 ps and variable delays after excitation. Time reference was provided by a fast photodiode which monitored a small fraction of the incident laser beam. Temporal measurements were recorded by coupling the optical fiber with a fast phototodiode connected to a 13 GHz bandwidth digital oscilloscope (Agilent Infiniium DSA91304A). In this case, the temporal response was limited by the 100 ps detector resolution.

3. RESULTS AND DISCUSSION

The laser-like effects of two different powder random laser samples A and B containing Rh6G doped SiO_2 nanoparticles are investigated. An experimental survey around the random laser threshold in both organic-inorganic hybrid materials, followed by theoretical results obtained with a light diffusive propagation model are detailed below.

3.1 Experimental results

Spectral and temporal emission characteristics such as linewidth and threshold behaviors were studied in a backscattering arrangement (Fig. 2) in samples A and B after picosecond optical pumping in single shot measurements. Figure 3(a) shows the normalized emission spectra obtained from the 2% Rh6G-SiO_2 nanoparticles dispersed within silica nanoparticles (sample A) when pumped with excitation pulse energies of 30, 74, 90 and 1800 μJ/pulse. At the lowest excitation energy the emission spectrum shows the typical broad fluorescence band of Rh6G. However, as the pump energy is increased the linewidth is reduced due to the rise of a gain-narrowed peak centered at 556.5 nm which

reveals the appearance of laser-like emission. At 1800 μJ/pulse the photoluminescence is completely suppressed and only the gain-narrowed peak survives (see thick full line of Fig. 3(a)). Fig. 3(b) shows the effective linewidth ($\Delta\lambda_{eff} = \int \frac{I(\lambda)d\lambda}{I_{\max}}$) collapse found in sample A from 51.8 nm to 11 nm.

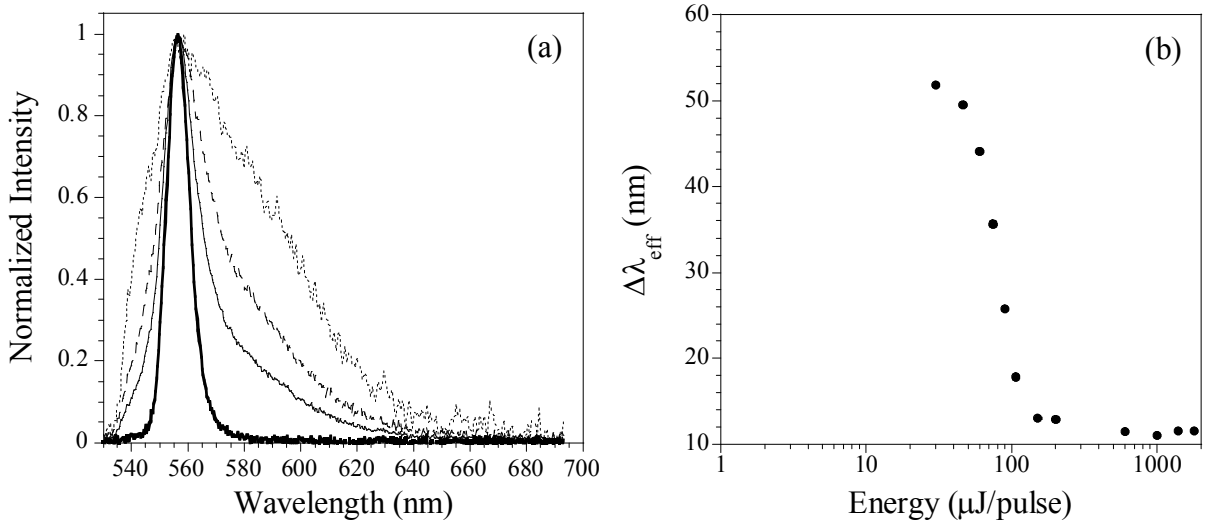

Fig. 3. (a) Normalized emission spectra of the 2% Rh6G-SiO_2 nanoparticles dispersed in silica powder obtained at 30 μJ/pulse (point line), 74 μJ/pulse (dashed line), 90 μJ/pulse (thin full line) and 1800 μJ/pulse (thick full line). (b) Pump energy dependence of the corresponding emission linewidths.

Figure 4(a) shows the normalized emission spectra obtained in the ground powder of a silica gel containing 2% Rh6G-SiO_2 nanoparticles (sample B) at 19, 25, 37, and 748 μJ/pulse. It is important to note that in this sample the fluorescence band of Rh6G peaks at 616 nm (point line in Fig. 4(a)) whereas the corresponding Rh6G spontaneous emission band is centered at 556.5 nm in sample A (point line in Fig. 3(a)). Redshifts of the Rh6G emission have been previously observed in sol-gel silica matrices as a function of dye concentration [26]. The redshift observed in this kind of matrices had been interpreted in two different ways: either due to the formation of aggregates [27] or to the presence of re-absorption phenomena [28]. As it will be later explained, lifetime measurements yield some additional evidences about the origin of the observed redshift.

Figure 4(b) presents the emission linewidth narrowing found in sample B as a function of the pump pulse energy. These experimental data indicate that the ground powder also acts as an efficient enough light scatter in the spectral range of the Rh6G optical gain. Note that the corresponding bulk dye doped silica gel is transparent at daylight so it is necessary to obtain ground powder out of it to give the scattering effect required for random lasing.

On the other hand, in sample A the broad spontaneous emission of Rh6G is observed when pumping with excitation energies up to 30 μJ/pulse (see point line in Fig. 3(a)). In contrast, at this pump energy a reduction of the emission linewidth of sample B already occurs (see Fig. 4), which indicates an important contribution of the stimulated emission to the corresponding emission spectra. Experimental data depicted in Figs. 3 and 4 thus demonstrate that no embedding medium for the Rh6G-SiO_2 nanoparticles is required to achieve random lasing. Nevertheless, a significant reduction of the laser threshold (defined as the energy value above which a suddenly drop of the spectral linewidth occurs) is found in the ground powder of the silica gel containing the fluorescent nanoparticles (~75 μJ/pulse and ~24 μJ/pulse for samples A and B, respectively).

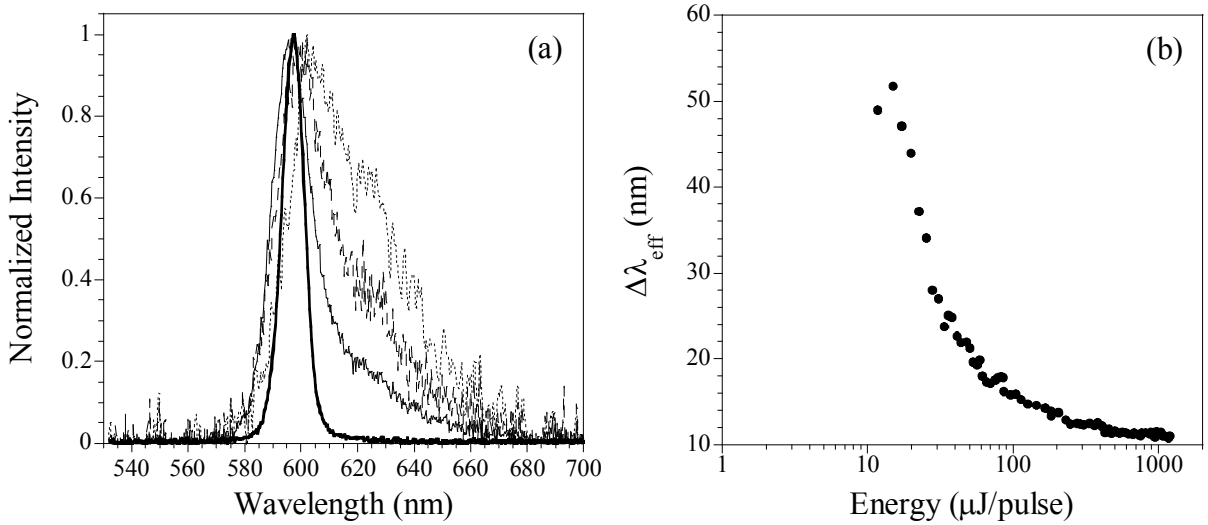

Fig. 4. (a) Normalized emission spectra of the ground powder of a bulk silica gel containing 2% Rh6G-SiO_2 nanoparticles obtained at 19 μJ/pulse (point line), 25 μJ/pulse (dashed line), 37 μJ/pulse (thin full line) and 748 μJ/pulse (thick full line). (b) Pump energy dependence of the corresponding emission linewidths.

Time-resolved spectroscopy measurements were also carried out around the onset of the laser-like action. It is worthy to notice that this is the only experimental technique which allows us to separate the narrow laser-like contribution to the emission spectrum from the spontaneous emission present when exciting around the threshold, and it therefore provides a detailed insight into the emission dynamics of the random laser sample. This is possible due to the different characteristic time scales involved in both processes. As an example, Fig 5(a) shows the emission spectra of sample B measured after excitation with 27.8 μJ single shot pulses, by using a 200 ps gate width, and delays of 0 ns, 0.5 ns, 0.75 and 1.3 ns. This figure evidences the different emission bandshapes obtained at variable delays in sample B. Stimulated emission, which in this case has a maximum net gain in a narrow spectral region around 598 nm, appears at the shortest time exposure and delays (see the two upper curves in Fig. 5(a)). At time delays longer than 0.5 ns, a broader and weaker emission band is observed, exhibiting the dominant photoluminescence contribution to the emission spectrum (see the two lower curves in Fig. 5(a)). Figure 5(b) thus shows the enhancement of the effective emission linewidth found in sample B as time delay is increased. On the other hand, the spontaneous emission of this sample is completely suppressed above a time delay of 1.8 ns. This result agrees well with the lifetime of Rh6G measured in sample B at low excitation energies (1.65 ns).

Temporal characteristics of the pulse emitted from samples A and B were also investigated by single shot measurements. Figure 6(a) compares the normalized emission decays of Rh6G measured at 20, 60, 90 and 1800 μJ/pulse in the 2% Rh6G-SiO_2 nanoparticles dispersed in a silica powder. At the lowest excitation energies the output pulse duration is limited by the lifetime of the Rh6G dye in this sample (4 ns) (see point line of Fig. 6(a)). However, a marked shortening of the output pulse is observed when increasing the pump energy (see Fig. 6(a) and 6(b)). In particular, the full width at half maximum (FWHM) of the time profile was reduced down to around 100 ps above the lasing threshold (see Fig. 6(b)). This is the actual time resolution of the detector we used to perform this set of measurements, so our real temporal width might be much narrower. As a matter of fact, studies on liquid dye and polymer sheet random lasers have given emission pulses as short as 50 ps [17] or even less [15,16].

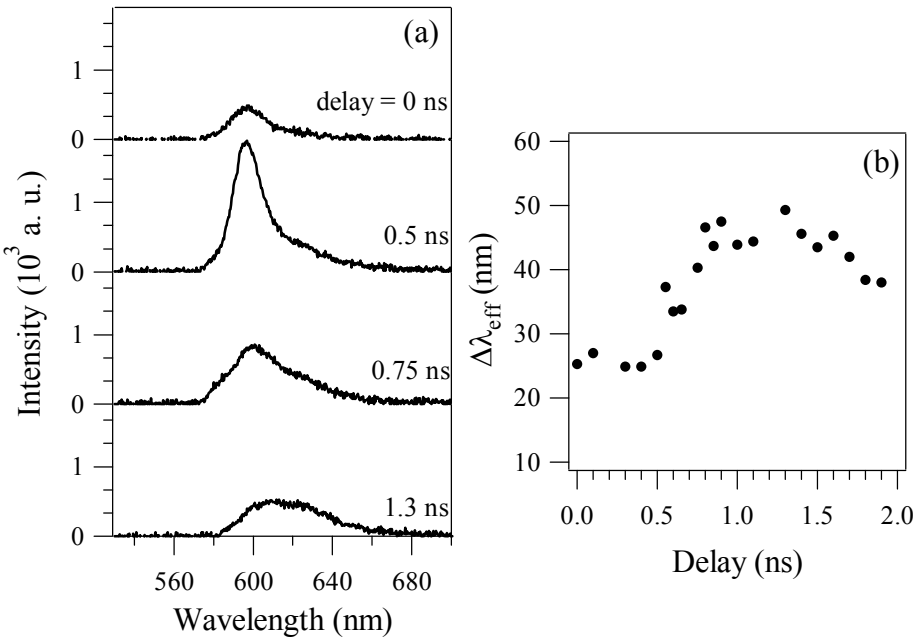

Fig. 5. (a) Emission spectra of the ground powder of a bulk silica gel containing 2% Rh6G-SiO_2 nanoparticles obtained at variable delays after excitation with 27.8 μJ/pulse energy. The exposure time was 200 ps. (b) Linewidths obtained at 27.8 μJ/pulse energy as a function of the time delay in this sample.

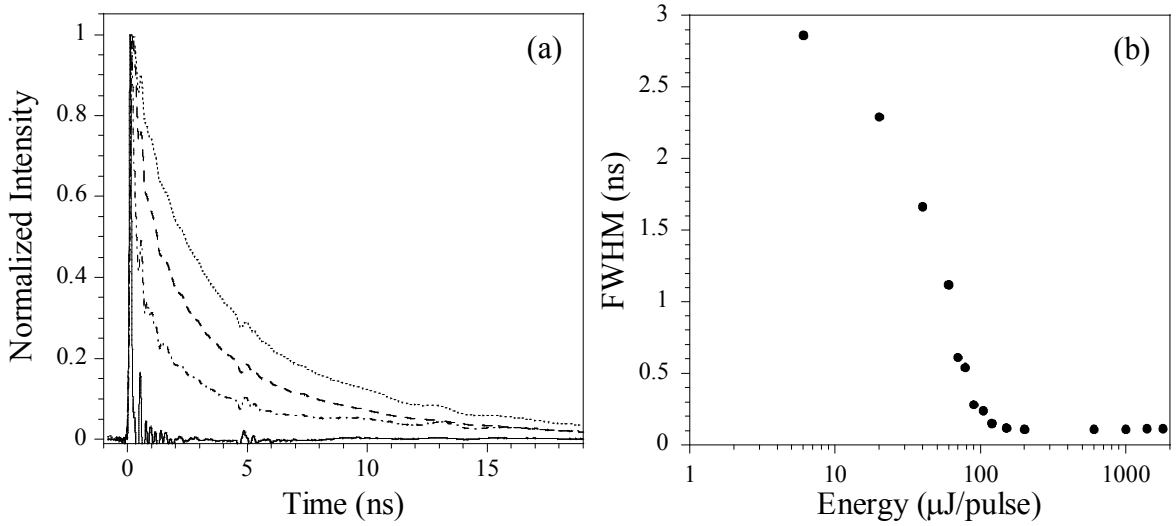

Fig. 6. (a) Normalized temporal profiles of the 2% Rh6G-SiO_2 nanoparticles dispersed in silica powder obtained at 20 μJ/pulse (point line), 60 μJ/pulse (dashed line), 90 μJ/pulse (dash-dot line) and 1800 μJ/pulse (full line). Their wavy structure is due to the typical response of the fast photodiode used in the experimental set-up. (b) FWHM of the corresponding time profiles as a function of the pump energy.

Figure 7(a) shows the temporal profile of sample B obtained at different excitation energies. There one sees that at low excitation energies the emission decay of Rh6G in this sample is faster than in sample A (compare with Fig. 6(a) and notice the different time scales). As we mentioned, a lifetime of 4 ns was found in sample A whereas the lifetime value measured in sample B is 1.65 ns. This lifetime quenching is a clear fingerprint not to assign the redshift found in the fluorescence spectrum of the later sample to re-absorption, for this case a lifetime increase would be expected due to

radiation trapping. So instead, the formation of aggregates in sample B seems to be a more adequate explanation to account for both experimental results. This would introduce new non-radiative de-activation channels (such as energy transfer processes from monomers to dimmers [29]) leading to a lifetime shortening. Note that in our two powder laser samples the dye doped nanoparticle concentration is the same. However, it is rather possible that the actual Rh6G concentration be higher in sample B than in A which could favor the formation of aggregates in the first case, as one has to bear in mind that a dye leakage is expected in the final preparation step of sample A due to the method employed for the dispersion in solution of the pure SiO_2 particles and the fluorescent nanoparticles.

The normalized emission decays of sample B obtained at 15.7, 19 and 169 μJ/pulse show the corresponding reduction of the output pulse duration in this sample. The resulting sharp FWHM drop of the output pulse is depicted in Fig. 7(b) as a function of the pump energy. A minimum time-width of 100 ps was also found in this case. Nevertheless a smaller pump pulse energy value is required to achieve this pulse duration due to the three times smaller lasing threshold of this sample if compared to sample A.

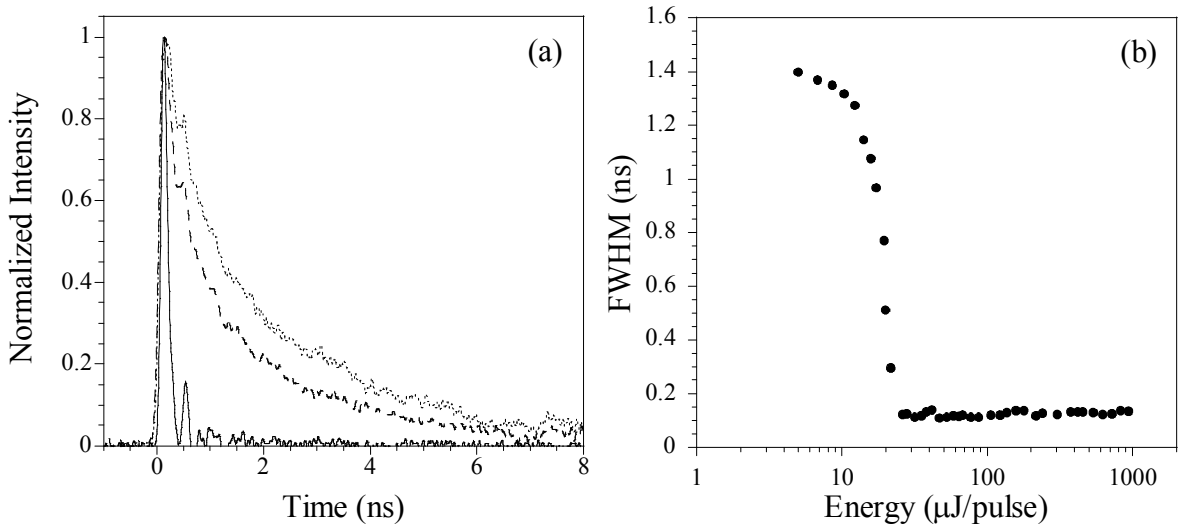

Fig. 7. (a) Normalized temporal profiles of the ground powder of a bulk silica gel containing 2% Rh6G-SiO_2 nanoparticles obtained at 15.7 μJ/pulse (point line), 19 μJ/pulse (dashed line) and 169 μJ/pulse (thin full line). Their wavy structure is due to the typical response of the fast photodiode used in the experimental set-up. (b) FWHM of the corresponding time profiles as a function of the pump energy.

Finally, the susceptibility to optical damage of sample B was investigated under VIS laser pulse irradiation. Almost no change is observed in the integrated emission intensity obtained when pumping at 100 μJ/pulse after an irradiation time of two hours which proofs its good photostability.

3.2 Theoretical calculations

We have performed theoretical calculations to study the laser emission dynamics of sample B which seems to be the most attractive one for potential future applications due to its lowest lasing threshold. In such an active ground powder the amount of scattering can be easily varied by changing the particle size in the grinding process. The average particle size of sample B provides mean free paths in the scattering medium which are much larger than the wavelength (l_t = 9.5 μm at 656 nm) and, consequently, the condition for the diffusion approximation is satisfied in this case ($\lambda << l_t << L$, where L is the scattering sample thickness). Our theoretical results have been obtained within this approximation which has been previously used to successfully analyze the behavior of several random lasers [6,7,16,30,31]. In particular, the following generalized time-dependent random laser equations were numerically solved by the Crank-Nicholson finite difference method (Δz = 0.05 μm, Δt = 10 ps) at the pump and emission wavelengths (λ_p = 532 nm and λ_e = 598 nm respectively):

$$\frac{\partial W_p(z,t)}{\partial t} = D_p \frac{\partial^2 W_p(z,t)}{\partial z^2} - \frac{D_p}{l_{abs}^2} W_p(z,t) + p(z,t) \tag{1}$$

$$\frac{\partial W_e(z,t)}{\partial t} = D_e \frac{\partial^2 W_e(z,t)}{\partial z^2} + f\,\mathrm{v}\sigma_{em} N(z,t) W_e(z,t) + \beta \frac{N(z,t)}{\tau_s} \tag{2}$$

$$\frac{\partial N(z,t)}{\partial t} = f\,\mathrm{v}K_{abs} W_p(z,t) - f\,\mathrm{v}\sigma_{em} N(z,t) W_e(z,t) - \frac{N(z,t)}{\tau_s} \tag{3}$$

$W_{p,e}(z,t)$ are the pump and emission light densities, $N(z,t)$ is the density of the dye molecules in the excited state, v = c/n_{eff} is the light speed in the medium where n_{eff} is the effective refractive index, σ_{em} is the stimulated emission cross section, τ_s is the excited state lifetime, and K_{abs} is the absorption coefficient of the material at the pump wavelength. $l_{abs} = \sqrt{\frac{l_t l_i}{3}}$ and $D = \frac{\mathrm{v} l_t}{3}$ are the diffusive absorption length and the light diffusion coefficient (D_p corresponds to the pump and D_e to the emitted radiation). The definitions of the mean free path lengths involved in the scattering and absorption processes are given elsewhere [24]. β is the fraction of spontaneous emission contributing to the laser process. f is the volume fraction occupied by the scatterers. *p(z,t)*, is the source of diffuse radiation which corresponds to a Gaussian pulse incoming the sample in the z direction and extinguished (scattered and absorbed) along the scattering path. The input values for the calculation are the material parameters: $\sigma_{em} = 2.5\text{x}10^{-16}$ cm^2, $\tau_s = 1.65$ ns, K_{abs} (532 nm) = 148.5 cm^{-1}, $n_{eff} = 1.16$, $f = 0.43$. The effective refractive index has been calculated by using the Maxwell-Garnet theory whereas the mean free paths at the required wavelengths (λ_p = 532 nm and λ_e = 598 nm) have been calculated by using the Mie theory for spheres in the independent-scatterer approximation with a diameter equal to the averaged mean particle size (ϕ = 3 μm). Based on the agreement found between the value for l_t calculated from this theory at 656 nm and the one experimentally obtained, Mie theory seems to be reliable for this purpose.

Figure 8(a) shows the excited-state populations and the temporal profiles of the emitted light obtained by using this laser model at 0.15, 60.8, 85.2, and 185.5 μJ/pulse. These curves have been normalized for the sake of comparison.

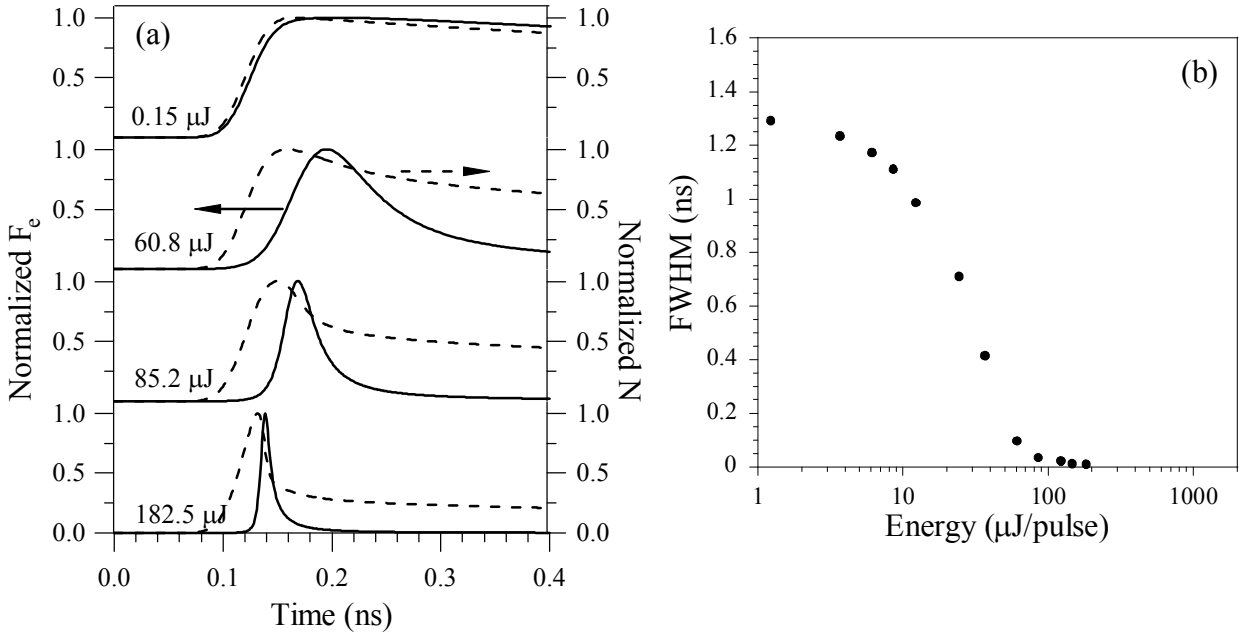

Fig. 8. (a) Normalized time profiles (F_e, solid lines) and excited-state populations (N, dashed line) calculated for $\beta = 0.5$ at 0.15, 60.8, 85.2 and 182.5 μJ/pulse by using the laser model described in Sec. 3.2 (b) FWHM of the simulated time profiles as a function of the pump pulse energy.

The time evolution of the emitted light is given by $\vec{F}_e = -D_e \frac{\partial W_e}{\partial z}\vec{z}$ evaluated at the sample surface ($z = 0$). This figure shows the theoretical pulse shortening predicted by our model as the excitation energy is increased. In fact, the FWHM of the output pulse is reduced from 1.31 ns to 12 ps (see Fig. 8(b)). From Fig. 8(b) a theoretical threshold of 24 μJ/pulse is obtained. It is worthy to notice that although the experimental pulse width is limited by the actual time resolution of the detector, and, therefore a larger experimental pulse duration is obtained at high energies, the theoretical and experimental FWHM collapse around the same energy value (compare Fig. 7(b) and 8(b)).

On the other hand, the build-up of the laser-like emitted pulse can be interpreted in the framework of ordinary Q-switch laser theory account taken of the formal similarity between our "laser equations" and the ones proposed by Florescu & John [32]. Moreover, following Ref. [32], our equations can be reduced to the basic Q-switch laser equations $\frac{dW_e}{dt} = \mathrm{v}\sigma_{em} N W_e - \gamma_c W_e$, $\frac{dN}{dt} \approx -2\mathrm{v}\sigma_{em} W_e N$ during the pulse build-up time [33]. Here, N is the population difference density, and γ_c the "cavity" decay rate which is related to the diffusion coefficient by $\gamma_c \equiv D_e / l_z^2$, where $l_z \cong 3l_{abs}$ [34,35]. A "cavity" decay time $\tau_c = 1/\gamma_c$ of 5.5 ps is thus obtained for our system. This value is close to the one given by the Q-switch theory, 6.4 ps, obtained from the time-dependence of N around the threshold and the output pulse width [33].

In Fig. 9, the integrated intensity of the output pulses measured in sample B as a function of the excitation energy is plotted (dots). The dashed line represents the linear fit to the experimental data. It provides a laser threshold around 24 μJ/pulse which agrees well with the theoretical estimation given above. The solid curve represents the theoretically calculated input-output curve obtained from numerical integrations of the temporal profiles for $\beta = 0.5$. As can be seen in this figure, it perfectly follows the experimental behavior of sample B.

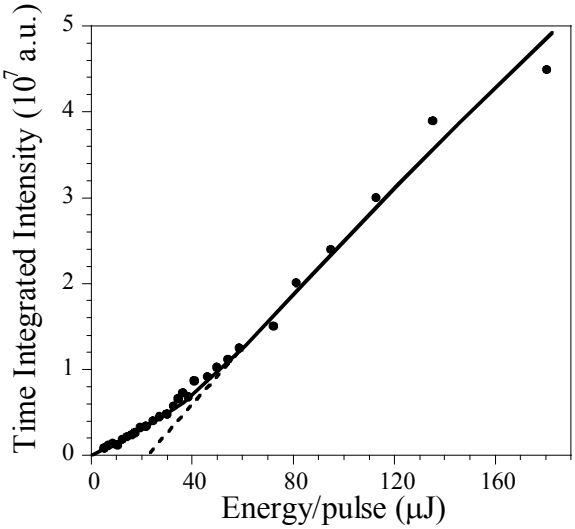

Fig. 9. (a) Integrated intensity of the output pulses obtained as a function of the pump pulse energy in the ground powder of a bulk silica gel containing 2% Rh6G-SiO_2 nanoparticles. The solid line represent the simulated data for $\beta = 0.5$. A laser threshold of 24 μJ/pulse is estimated from the linear fit (dashed line) of the experimental data (dots).

4. CONCLUSIONS

We have observed and characterized random laser-like effects such as spectral narrowing, emission intensity increase and pulse shortening in two different and novel solid-state samples synthesized by the sol-gel technique. Both novel organic-inorganic hybrid materials contain Rh6G doped SiO_2 nanoparticles which are either dispersed within pure silica particles (sample A) or embedded in a silica gel matrix which is subsequently ground (sample B). The experimental

results obtained in these powder laser systems show parallel behaviors in spectral and time domains as a function of the pumping energy and demonstrate that the lasing threshold is significantly reduced when the fluorescent nanoparticles are embedded in a gel silica matrix and ground powder is obtained out of it (~ 75 μJ/pulse and 24 μJ/pulse for sample A and B, respectively). In this case, a redshift of the Rh6G fluorescence emission and a lifetime quenching are found when exciting below the onset of laser-like action. This could be ascribed to the presence of dye aggregates due to a higher Rh6G dye concentration in sample B.

On the other hand, experimental data concerning the laser-like emission dynamics of sample B are compared with theoretical results obtained within diffusive conditions of light propagation by using a laser model with a feedback provided by the ground powder. We have found both good qualitative and quantitative agreements for the pulse duration collapse and laser threshold. The behavior of this system is close to a classical Q-switched laser under ultrashort pumping.

Finally we believe that the present solid-state dye doped systems turn out to be very attractive materials for any potential device utilizing the random lasing phenomenon due to their low lasing threshold and good photostability.

ACKNOWLEDGMENTS

This work has been supported by the Spanish Government MEC under Projects No. MAT2008-05921/MAT, NAN2004-09317-C04-02, Consolider SAUUL CSD2007-00013 and Basque Country Government (IT-331-07). S. G.-R. acknowledges financial support from the Spanish MEC under the "Juan de la Cierva" program. The authors are grateful to Dr. M. Al-Saleh for his assistance and to B. García-Ramiro and Dr. M.A. Illarramendi for their contribution in the modelling.

REFERENCES

[1] Letokhov, V. S., "Stimulated emission of an ensemble of scattering particles with negative absorption," JETP Lett. 5, 212-215 (1967).
[2] Wiersma, D. S., "The physics and applications of random lasers," Nature Physics 4, 359-367 (2008).
[3] Noginov, M. A., [Solid-State Random Lasers], Springer, Berlin, (2005)
[4] Cao, H., "Lasing in random media," Waves Random Media 13, R1-R39 (2003).
[5] Mujumdar, S., Turck, V., Torre, R. and Wiersma, D. S., "Chaotic behavior of a random laser with static disorder," Phys. Rev. A 76, 033807 (2007).
[6] John, S. and Pang, G., "Theory of lasing in a multiple-scattering medium," Phys. Rev. A 54(4), 3642-3652 (1996).
[7] Wiersma, D. S. and Lagendijk, A., "Light diffusion with gain and random lasers," Phys. Rev. E 54(4), 4256-4265 (1996).
[8] Jiang, X. and Soukoulis, C. M., "Time dependent theory for random lasers," Phys. Rev. Lett. 85(1), 70-73 (2000).
[9] Burin, A. L., Ratner, M. A., Cao, H. and Chang, R. P. H., "Model for a random laser," Phys. Rev. Lett. 87, 215503 (2001).
[10] van der Molen, K. L., Mosk, A. P. and Lagendijk, A., "Quantitative analysis of several random lasers," Opt. Commun. 278, 110-113 (2007).
[11] Ferjani, S., Barna, V., De Luca, A., Versace, C. and Strangi, G., "Random lasing in freely suspended dye-doped nematic liquid crystals," Opt. Lett. 33(6), 557-559 (2008).
[12] Lawandy, N. M., Balachandran, R. M., Gomes, A. S. L. and Sauvain, E., "Laser action in strongly scattering media," Nature 368, 436-438 (1994).
[13] Anglos, D., Stassinopoulos, A., Das, R. N., Zacharakis, G., Psyllaki, M., Jakubiak, R., Vaia, R. A., Giannelis, E. P. and Anastasiadis, S. H., "Random laser action in organic-inorganic nanocomposites," J. Opt. Soc. Am. B 21(1), 208-213 (2004).
[14] Wang, H. Z., Zhao, F. L., He, Y. J., Zheng, X. G., Huang, X. G. and Wu, M. M., "Low-threshold lasing of a Rhodamine dye solution embedded with nanoparticle fractal aggregates," Opt. Lett. 23(10), 777-779 (1998).
[15] Sha, W. L., Liu, C. H. and Alfano, R. R., "Spectral and temporal measurements of laser action of Rhodamine 640 dye in strongly scattering media," Opt. Lett. 19(23), 1922-1924 (1994).

[16] Siddique, M., Alfano, R. R., Berger, G. A., Kempe, M. and Genack, A. Z., "Time-resolved studies of stimulated emission from colloidal dye solutions," Opt. Lett. 21(7), 450-452 (1996).
[17] Zacharakis, G., Heliotis, G., Filippidis, G., Anglos, D. and Papazoglou, T. G., "Investigation of the laserlike behavior of polymeric scattering gain media under subpicosecond laser excitation," Appl. Opt. 38(28), 6087-6092 (1999).
[18] Lee, C. W., Wong, K. S., Huang, J. D., Frolov, S. V. and Vardeny, Z. V., "Femtosecond time-resolved laser action in poly(p-phenylene vinylene) films: stimulated emission in an inhomogeneously broadened exciton distribution," Chem. Phys. Lett. 314, 564-569 (1999).
[19] Shin, H. W., Cho, S. Y., Choi, K. H., Oh, S. L. and Kim, Y. R., "Directional random lasing in dye-TiO_2 doped polymer nanowire array embedded in porous alumina membrane," Appl. Phys. Lett. 88, 263112 (2006).
[20] Zhang, D., Wang, Y. and Ma, D., "Random lasing emission from a red fluorescent dye doped polystyrene film containing dispersed polystyrene nanoparticles," Appl. Phys. Lett. 91, 091115 (2007).
[21] Frolov, S. V., Vardeny, Z. V., Zakhidov, A. A. and Baughman, R. H., "Laser-like emission in opal photonic crystals," Opt. Commun. 162, 241-246 (1999).
[22] Gottardo, S., Sapienza, R., García, P. D., Blanco, A., Wiersma, D. S. and Lopez, C., "Resonance-driven random lasing," Nature Photon. 2, 429-432 (2008).
[23] García-Revilla, S., Fernández, J., Illarramendi, M. A., García-Ramiro, B., Balda, R., Cui, H., Zayat, M. and Levy, D., "Ultrafast random laser emission in a dye-doped silica gel powder," Opt. Express 16(16), 12251-12263 (2008).
[24] García-Ramiro, B., Illarramendi, M. A., Aramburu, I., Fernández, J., Balda, R. and Al-Saleh, M., "Light propagation in optical crystal powders: effects of particle size and volume filling factor," J. Phys.: Condens. Matter 19(45), 456213 (2007).
[25] Illarramendi, M. A., Aramburu, I., Fernández, J., Balda, R., Williams, S. N., Adegoke, J. A. and Noginov, M. A., "Characterization of light scattering in translucent ceramics," J. Opt. Soc. Am. B 24(1), 43-48 (2007).
[26] Anedda, A., Carbonaro, C. M., Corpino, R., Ricci, P. C., Grandi, S. and Mustarelli, P. C., "Formation of fluorescent aggregates in Rhodamine 6G doped silica glasses," J. Non-Crys Sol. 353, 481-485 (2007).
[27] Del Monte, F., Mackenzie, J. D. and Levy, D., "Rhodamine fluorescent dimers adsorbed on the porous surface of silica gels," Langmuir 16, 7377-7382 (2000).
[28] Hungerford, G., Suhling, K. and Ferreira, J. A., "Comparison of the fluorescence behaviour of Rhodamine 6G in bulk and thin film tetraethylorthosilicate derived sol-gel matrices," J. Photochem. Photobiol. A 129, 71 (1999).
[29] Narang, U., Bright, F. V. and Prasad, P. N., "Characterization of Rhodamine 6G-doped thin sol-gel films," Appl. Spectroscopy 47(2), 229-234 (1993).
[30] Genack, A. Z., "Optical transmission in disordered media," Phys. Rev. Lett. 58(20), 2043-2046 (1987).
[31] Berger, G. A., Kempe, M. and Genack, A. Z., "Dynamics of stimulated emission from random media," Phys. Rev. E 56(5), 6118-6122 (1997).
[32] Florescu, L. and John, S., "Lasing in a random amplifying medium: Spatiotemporal characteristics and nonadiabatic atomic dynamics," Phys. Rev. E 70, 036607 (2004).
[33] Siegman, A. E., [Lasers], Mill Valley, California, (1986)
[34] van Soest, G., Poelwijk, F. J., Sprik, R. and Lagendijk, A., "Dynamics of a random laser above threshold," Phys. Rev. Lett. 86(8), 1522-1525 (2001).
[35] Balachandran, R. M. and Lawandy, N. M., "Theory of laser action in scattering gain media," Opt. Lett. 22(5), 319-321 (1997).